INTERNATIONAL
SOIL AND WATER
CONSERVATION RESEARCH

Using meshes to change the characteristics of simulated rainfall produced by spray nozzles

Sílvia C. P. Carvalho[1], João L. M. P. de Lima[2], and M. Isabel P. de Lima[3]

Abstract

Rainfall simulators have been used for many years contributing to the understanding of soil and water conservation processes. Nevertheless, rainfall simulators' design and operation might be rather demanding for achieving specific rainfall intensity distributions and drop characteristics and are still open for improvement. This study explores the potential of combining spray nozzle simulators with meshes to change rainfall characteristics, namely drop properties (drop diameters and fall speeds). A rainfall simulator laboratory set-up was prepared that enabled the incorporation of different wire meshes beneath the spray nozzles. The tests conducted in this exploratory work included different types of spray nozzles, mesh materials (plastic and steel), square apertures and wire thicknesses, and positions of the meshes in relation to the nozzles. Rainfall intensity and drop size distribution and fall speed were analysed. Results showed that the meshes combined with nozzles increased the mean rainfall intensity on the 1 m^2 control plot below the nozzle and altered the rain drops' properties, by increasing the mass-weighted mean drop diameter, for example.

Key Words: Rainfall simulators, Spray nozzle, meshes, Drop characteristics

1 Introduction

Rainfall simulation is a common tool that has been widely used in studies related to soil erosion, nutrient and pollutant transport, water conservation and agricultural management practices. One of the main advantages of rainfall simulation is the possibility to generate and replicate rainfall with a specific intensity and duration (e.g. de Lima and Singh, 2003; Potter et al., 2006; de Lima et al., 2013). In laboratory controlled conditions, it is also possible to reduce the effects of the variability of temperature, humidity and wind, as experienced in the field (e.g. de Lima et al., 2003; Fister et al., 2012). Nevertheless, rainfall simulators' design is demanding, raising questions on rainfall distribution and intensity, drop characteristics, manpower required, energy availability, costs and transportability.

In the literature, one finds many studies that have used rainfall simulators. These include studies by Mutchler and Hermsmeier (1965), de Ploey (1981), Bowyer-Bower and Burt (1989), and de Lima et al. (2003, 2008). However, the rainfall simulators' drop properties and spatial intensity distribution is often not discussed (e.g. Lascelles et al., 2000; Ries et al., 2009) although some studies report on the mean drop size of the simulated rain (e.g. Arnaez et al., 2007; Marques et al., 2007). In natural rain, large mean drop sizes are associated with high rain intensities, but in simulated rain the relationship between drop size and intensity may be different. For example, Parsons and Stone (2006) reported simulated intensities ranging from 59 to 170 mm h^{-1}, but the median drop size remained constant at 1.2 mm.

Rain simulators can be classified according to the way they produce drops. The two most common types of

[1] M.Sc., Department of Civil Engineering, Faculty of Science and Technology, University of Coimbra, Coimbra, Portugal. E-mail: silviacc@student.dec.uc.pt

[2] Prof., Department of Civil Engineering, Faculty of Science and Technology, University of Coimbra, Coimbra, Portugal. Corresponding author: João L. M. P. de Lima, Department of Civil Engineering, Campus II – University of Coimbra, Rua Luís Reis Santos, 3030-788 Coimbra, Portugal. Tel.:+351 239 797 183; fax: +351 239 797 179; E-mail: plima@dec.uc.pt

[3] Assist. Prof., Department of Civil Engineering, Faculty of Science and Technology, University of Coimbra, Coimbra, Portugal. E-mail: iplima@uc.pt

simulators are: (i) non-pressurized rainfall simulators or drop-former simulators which drip water from hypodermic needles and capillary tubes (e.g. Munn and Huntington, 1976; Kamphorst, 1987; Abd Elbasit et al., 2010); (ii) pressurized rainfall simulators, such as spray nozzles (e.g. Meyer and McCune, 1958; Esteves et al., 2000).

Non-pressurized rainfall simulators are less used in the laboratory; but they are a convenient technique for places experiencing difficult access and limitations in water supply (e.g. Humphry et al., 2002). The well-known disadvantage in these simulators is that they produce a narrow range of drop sizes (e.g. Tossell et al., 1987) and a small drop fall speed. Some non-pressurized rainfall simulators include meshes below the drop formers in order to break up water drops into a distribution of drop sizes closer to that of natural rainfall and to randomize drop landing positions (e.g. Holden and Burt, 2002; Clarke and Walsh, 2007; Fernández-Gálvez et al., 2008).

Pressurized rainfall simulators have an important advantage over the non-pressurized simulators: drops do not rely on gravity to reach terminal velocity, but are sprayed under pressure. For example, the hydraulic spray nozzles, which are commonly used in scientific and technical experiments on soil and water conservation, operate by discharging the water under pressure through an exit orifice with a small diameter. This leads to an increase in water velocity, causing instability in the nozzle exit and subsequent breakup into small drops; typically a spray nozzle provides a broader range of drop sizes compared to non-pressurized simulators (e.g. Battany and Grismer, 2000). Moreover, drop properties and hence the entire simulated event will depend on the pressure applied, the flow rate, and the nozzle design (e.g. Kincaid, 1996; Cerdà et al., 1997; Erpul et al., 1998).

To our knowledge, meshes have been combined with drop-former simulators but not with nozzle type simulators. However, Schindler Wildhaber et al. (2012) recently described a "field hybrid simulator", and claimed that the performance of the simulator improved in relation to the mean drop size and kinetic energy when a mesh grid (aperture size of 2 mm × 1.7 mm) was fixed at a distance of 0.5 m under a spray nozzle.

The objective of this study was to further explore the effect of meshes on spray nozzle rain simulations, namely on rain intensity, drop size and drop fall speed. In particular, we are interested in the raindrop properties which are important for calculating rainfall erosivity. These properties depend on the design and operation of rainfall simulators.

2 Materials and methods

2.1 *Laboratory set-up*

Fig. 1 shows a schematic representation of the laboratory set-up used in this study. The main components are: the rainfall simulator which includes a downward-oriented spray nozzle operating in a static position; a

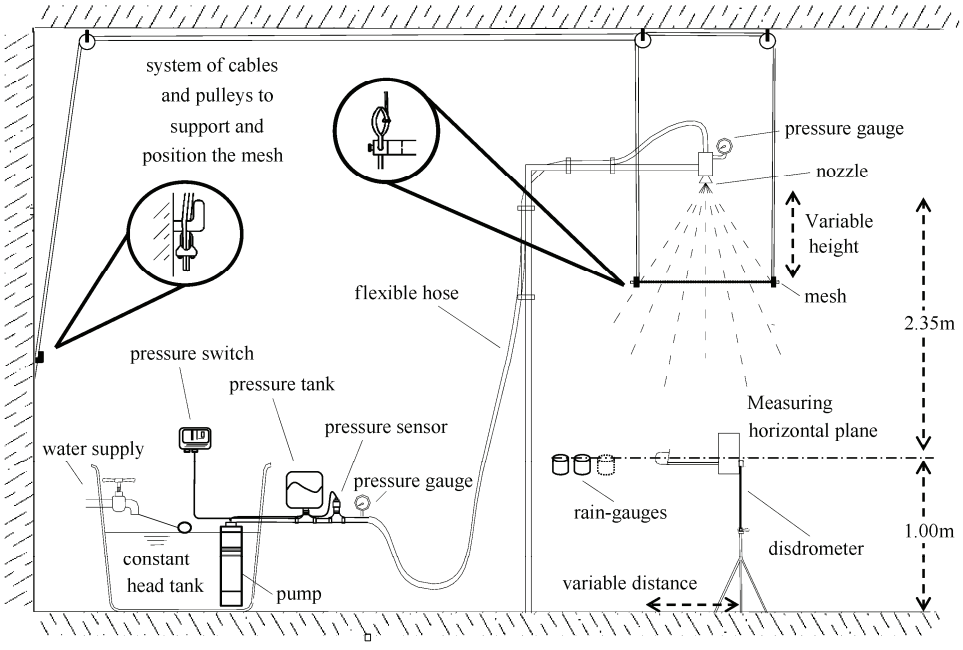

Fig. 1 Set-up of the laboratory experiments

mesh suspended by a system of cables and pulleys at variable vertical distances to the nozzle; and rainfall measuring devices, namely rain-gauges and a disdrometer. These measuring devices were set at 2.35 m below the nozzles, on an horizontal plane. The rainfall simulator installation also includes a constant head reservoir, a submersible pump, a pressure tank, a pressure sensor, two pressure gauges, a pressure switch, pipes and a flexible hose.

2.1.1 Nozzles

Four types of spray nozzles were used to simulate rainfall with different intensities and drop size distributions. The nozzles selected were single full-cone nozzles (HH-22, HH-14W and HH-4.3W) and a multiple full-cone nozzle (7G-1). All were manufactured by Spraying Systems Co. Table 1 gives a description of the spray nozzles used in the experiments, including the pressure at the nozzle, spray angle (i.e. angle of the water cone; see Fig. 2) and discharge. The pressure at the nozzle was kept constant at 1.5 bar for all the experiments. Spraying Systems Co. (2013) claims that the spray angle of the nozzles is higher at this pressure and that, in general, increasing operating pressure is expected to lead to decreasing drop sizes and increasing drop velocities.

Table 1 **Description of the spray nozzles used in the experiments. All nozzles are manufactured by Spraying Systems Co.**

Spray nozzle code	HH-22	HH-14W	HH- 4.3W	7G-1
Type	Full-cone spray nozzle: standard	Full-cone spray nozzle: wide angle		Fine spray nozzle (multiple full cone pattern)
Pressure (bar)	1.5	1.5	1.5	1.5
Discharge (L min^{-1})	11.9	7.6	2.3	4.3
Spray angle (º)	90	120	120	170

2.1.2 Meshes

The rain simulator was adapted to allow for the installation of meshes at different distances beneath the nozzles, with the purpose to change the characteristics of the simulated sprays. Thus, the set-up included a system of cables and pulleys that were used to support and position the meshes, which were stretched and attached to a 1 m^2 metal square frame. The main characteristics of the meshes used in the experiments are described in Table 2. The meshes had different square apertures and wire thicknesses, defining different percentages of open area in relation to the area of the frame. Since the adhesion and surface tension forces depend on the material, two materials were tested: steel and plastic.

Table 2 **Properties of the wire meshes used in the experiments**

Meshes	1	2	3	4	5	6
Material	Plastic (polyethylene and polypropylene)			Steel (welded wire)		
Square aperture (mm)	12	20	40	20	40	40
Weight (g m^{-2})	210	470	235	1,200	600	5500
Wire thickness (mm)	1.0 – 1.5	2.0 – 3.0	2.0 – 3.0	1.4	1.4	4.0
Open area (%)	82	79	89	87	93	83

2.1.3 Instrumentation

Characteristics of the nozzle sprays such as drop size and fall speed, and raindrop count over time were measured using a Laser Precipitation Monitor, manufactured by Thies Clima (e.g. Thies, 2007). The instrument includes a laser-optical source which produces a light-beam (infrared, 785 nm); in a receiver, the optical intensity is transformed into an electrical signal. When a rain drop falls through the light-beam (measuring area: 4,777 mm^2) the receiving signal is reduced. The diameter of the drop is calculated from the amplitude of the signal reduction and the drop fall speed is determined from the duration of the reduced signal. The disdrometer used in the laboratory yields the distribution of the raindrops over 21 diameter-size classes (from 0.125 mm to 8.000 mm) and 20 fall speed classes (up to 20.0 m s^{-1}). The class intervals do not all have the same width.

The rain intensity on the target surface was assessed using rain gauges with an opening diameter of 0.116 m,

corresponding to a collection area of 10,568 mm^2 (see section 2.2.2).

2.2 *Methodology*

The laboratory experiments were comprised of rain simulations from spray nozzles combined with meshes and spray nozzles only (i.e. the meshes were absent from the rain simulations). For these two cases, the simulated rainfall intensity and drop size and fall speed were examined. The laboratory procedures included: (1) selection of the nozzle and operating pressure of 1.5 bar; (2) selection of a mesh, which was positioned at a certain vertical distance from the nozzle; (3) start of the rainfall simulation; (4) rain measurements (rain gauges and disdrometer). We have undertaken the measurements defined in Table 3 and explained below.

Table 3 Summary of experiments using different combinations of nozzles and meshes

					Spray Nozzles							
	Material	Aperture (mm)	Thickness (mm)	Vertical distance to the nozzle (mm)	HH-22		HH-14W		HH-4.3W		7G-1	
					Rain gauges	Disdrometer	Rain gauges	Disdrometer	Rain gauges	Disdrometer	Rain gauges	Disdrometer
Meshes	Plastic	12	~1.25	200	✓	•	✓	•	✓	•	✓	•
				400	✓	•	✓	•	✓	•	✓	•
				600	✓	•	✓	•	✓	•	✓	•
		20	~2.5	200	✓	•	✓	•	✓	•	✓	•
				400	✓	•	✓	•	✓	•	✓	•
				600	✓	•	✓	•	✓	•	✓	•
		40	~2.5	600			✓	•				
	Steel	20	1.4	600			✓	•				
		40	4.0	600			✓	•				
		40	1.4	600			✓	•				
	without meshes				✓	•	✓	•	✓	•	✓	•

✓ 3 replicates; 15 rain gauges (5 rain gauges located on the control plot), see Fig. 3c.

• disdrometer in 3 positions, 3 replicates (sampling time was 15 seconds), see Fig. 3d.

Not measured.

2.2.1 Position of the meshes

The meshes were suspended at three positions: 200, 400 and 600 mm vertical distances below the nozzles. These three positions of the meshes are represented schematically in Fig. 2, which also shows the spray angle and the spray boundary for each nozzle, obtained for an operation pressure of 1.5 bar. This figure illustrates the expected interception of the sprays by the square meshes (1×1 m^2), which varies with the vertical distance between the meshes and the nozzles. At some positions the meshes are able to intercept the whole spray. The information on the nozzles' sprays was based on photographs captured during the experiments.

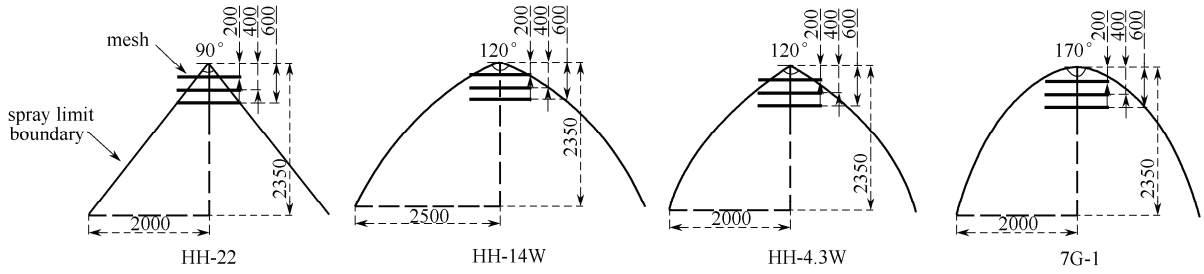

Fig. 2 Spray angle and spray limit boundary for the 4 nozzles used in the experiments (The 3 mesh positions beneath the nozzles are represented. The nozzle vertical distance to the target surface is 2.35 m; operating pressure is 1.5 bar; on the target surface, measures are for the wetted area. Distances are in mm.)

2.2.2 Rainfall intensities

A control square plot of 1 m^2 was used for assessing the simulated rainfall intensities on the target surface. This plot (horizontal measuring plane, in Fig. 1) was defined at a height of 1 m above the floor and at a vertical distance of 2.35 m below the nozzle, and was centered in relation to the nozzle position. We will refer to this area as "control plot". We noticed that this control plot size has been adopted in many soil and water conservation studies on small scale field plots that have used rainfall simulators.

The distribution of the simulated rainfall intensity on the control plot was evaluated with 41 rain-gauges scattered over the plot (Fig. 3a); the sampling interval for the rain measurements was three minutes and 3 replicates were undertaken. The uniformity of the distribution was assessed using the coefficient of uniformity (CU) defined by Christiansen (1941).

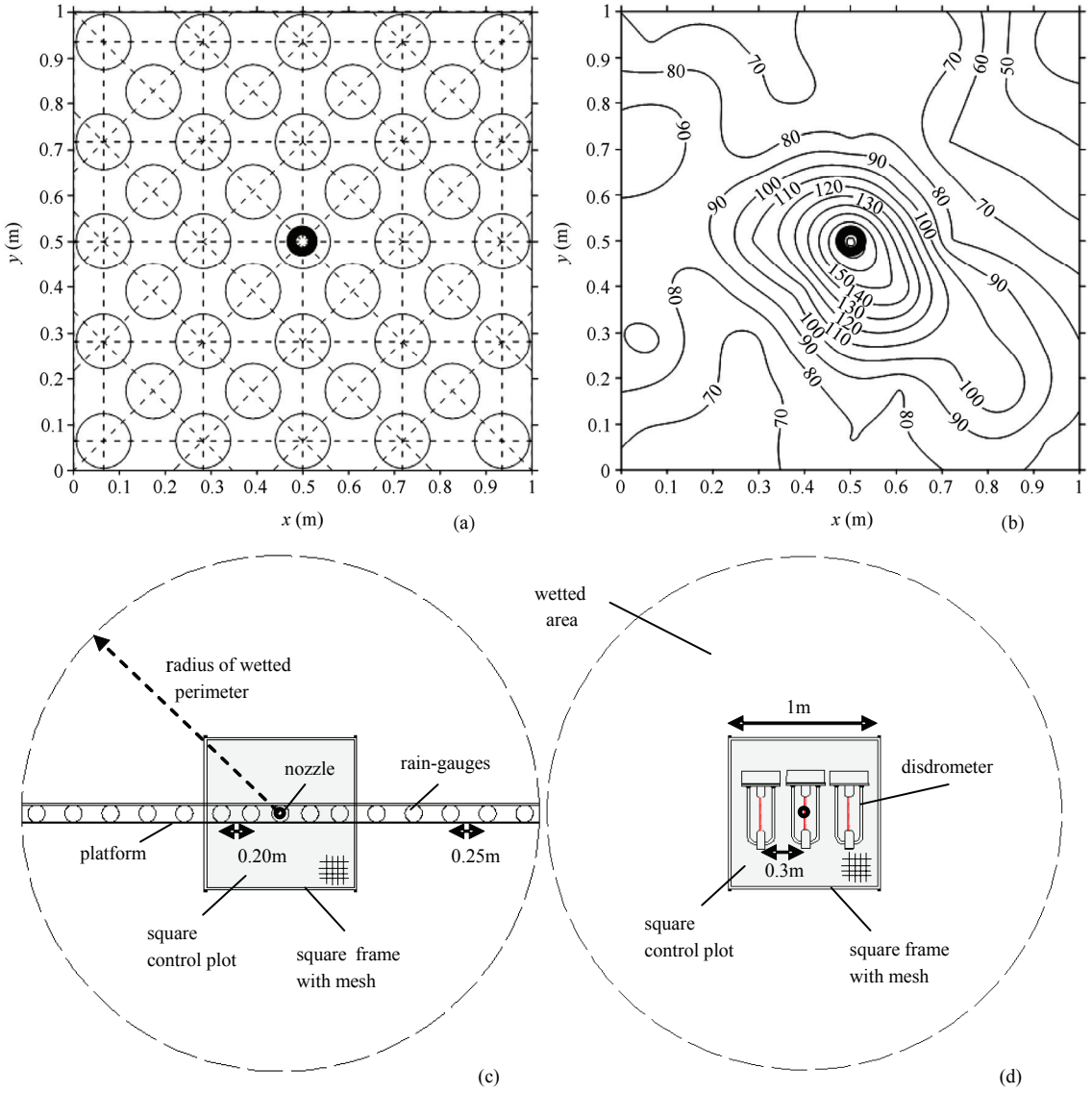

Fig. 3 (a) Position of the 41 rain-gauges used to measure the rainfall intensity on a 1 m^2 square plot (control plot, top view); (b) Spatial distribution of the simulated rainfall intensity [mm h^{-1}] under the 7G-1 nozzle, estimated using Kriging; (c) Position of 15 rain-gauges used to measure the rainfall intensity along a given direction (top view); (d) The position of the disdrometer used to measure drop properties (top view) (The black ring identifies the position of the nozzle.)

The laboratory work involved 32 experiments that included combinations of 4 nozzles with 6 meshes, positioned at 3 vertical distances from the nozzle (not all possible combinations were considered in this exploratory work; see Table 3). In addition, 3 replicates were carried out for each case. Because using a 41

rain-gauge grid for assessing the rainfall spatial distribution for all these cases would imply a great number of measurements, and because the rainfall intensity distribution was observed to be approximately symmetric (see Fig. 3b, for nozzle 7G-1), then the rainfall distribution on the target surface was estimated by studying the rain distribution along a single transect; this is illustrated in Fig. 3c that shows equally distributed rain-gauges set along a given direction defined on the wetted area, at the target surface level. Thus, estimates of rainfall intensity on the control plot used data from 5 rain-gauges, distributed along 1 m; and across the whole wetted area rain intensity was estimated using data from 15 rain-gauges that covered a 3.5 m distance (Fig. 3c).

2.2.3 Drop properties

Raindrop diameter and fall speed were recorded with a laser disdrometer, which was positioned with the light-beam coinciding with the target surface (i.e. measuring plane of the rain-gauges). Three measuring positions were adopted on this plane (Fig. 3d). Measurements' sampling time was 15 seconds; this small sampling time is explained by limitations of the disdrometer and its software in handling a large number of raindrops during the usual 1-minute resolution of the device, because counting limits of the number of particles were surpassed during the laboratory runs and the 1-minute data were then not reliable. So, to avoid exceeding the number of drops' counting limit we have restricted the observation time; we expect that the time variability in the simulations is small and that this procedure did not introduce important bias in the results; we nevertheless took 3 replicates of the measurements and calculated the mean. For each measurement the instrument provides a two dimensional matrix with the count of drops in each of the size and fall speed classes, which is used for determining the drop size distribution of the simulated rain.

The number and size of raindrops within a unit volume of air can be described by the number concentration, $N(D)$ ($mm^{-1}m^{-3}$), also called the raindrop size distribution (DSD), where D (mm) is the spherical equivalent diameter of each raindrop. The expected number of drops $N(D_i)$ ($mm^{-1}m^{-3}$) in the raindrop size class i [21 classes, with D_i (mm) being the central diameter of the size class i] is obtained by (e.g. Krajewski et al., 2006):

$$N(D_i) = \frac{1}{A\Delta t \Delta D_i} \sum_{j=1}^{20} \frac{n_{ij}}{v_j} \tag{1}$$

where n_{ij} is the number of detected raindrops in the size class i and belonging to the fall speed class j (20 classes) that is measured during the interval Δt (here is Δt=15 s, as explained above), v_j (m s^{-1}) is the fall speed of the raindrops at the middle of the fall speed class j, A (m^2) is the disdrometer detection area and ΔD_i (mm) is the width of the drop size class i.

The DSD can also be described in general by the mass-weighted mean drop diameter, D_m (mm), which is estimated using (e.g. Ulbrich, 1983):

$$D_m = \frac{\sum_{i=1}^{21} D_i^4 N(D_i) \Delta D_i}{\sum_{i=1}^{21} D_i^3 N(D_i) \Delta D_i} = \frac{\sum_{i=1}^{21} D_i^4 \left(\frac{1}{A\Delta t} \sum_{j=1}^{20} \frac{n_{ij}}{v_j}\right)}{\sum_{i=1}^{21} D_i^3 \left(\frac{1}{A\Delta t} \sum_{j=1}^{20} \frac{n_{ij}}{v_j}\right)} \tag{2}$$

The mean fall speed of the raindrops, v_m (m s^{-1}), is calculated by:

$$v_m = \frac{\sum_{j=1}^{20} n_j v_j}{N} \tag{3}$$

where n_j is the number of detected raindrops in the fall speed class j, v_j (m s^{-1}) is the central fall speed of the fall speed class j, and N is the total number of detected raindrops.

3 Results and discussion

This section is dedicated to exploring simulated rainfall intensities and drop properties. The control runs were for mesh free simulations (i.e. without combining nozzles and meshes).

3.1 *Rainfall intensities*

The distribution of the simulated rainfall intensity on the target surface (at 2.35 m below the nozzle; see section 2.2.2) were examined for different experimental runs (Table 3). We aimed at investigating the impact of the following variables on the simulated rain intensities:

i) *Nozzle type*: rainfall intensities simulated by different nozzles were compared, with each nozzle being combined with one plastic mesh (20 mm square aperture), and for 3 mesh positions;

ii) *Mesh position*: rainfall intensities obtained for 3 mesh positions were compared for combinations of 4 nozzles and 2 plastic meshes (12 mm and 20 mm square aperture);

iii) *Mesh characteristics*: rainfall intensities obtained using different mesh characteristics (material, aperture and wire thickness) were compared for rain simulated by one nozzle type (HH-14W) and the meshes positioned at one fixed position (i.e. at 600 mm vertical distance below the nozzle).

a) *Material*: the influence of the meshes' material on the simulated rain was studied by comparing the effects of 3 plastic meshes with those of 3 steel meshes.

b) *Aperture*: the effect of different meshes' apertures was studied by comparing the rainfall intensities obtained using plastic meshes with square aperture of 20 mm and 40 mm (both with ~2.5 mm wire thicknesses). The same effect was studied for the steel meshes with squares apertures of 20 mm and 40 mm (both with 1.4 mm wire thicknesses).

c) *Wire thickness*: the influence of the wire thicknesses was explored by comparing the impact of 40 mm square aperture steel meshes with wires of 1.4 mm and 4 mm thicknesses.

3.1.1 With and without combining the nozzles with meshes

The mesh-free rainfall simulations were compared with the rainfall altered by combining the four nozzles with plastic meshes of 20 mm square aperture, positioned at three different distances from the nozzles (200, 400 and 600 mm). Fig. 4a to d show the rain intensities observed along the 3.5 m diameter of the wetted area on the target surface.

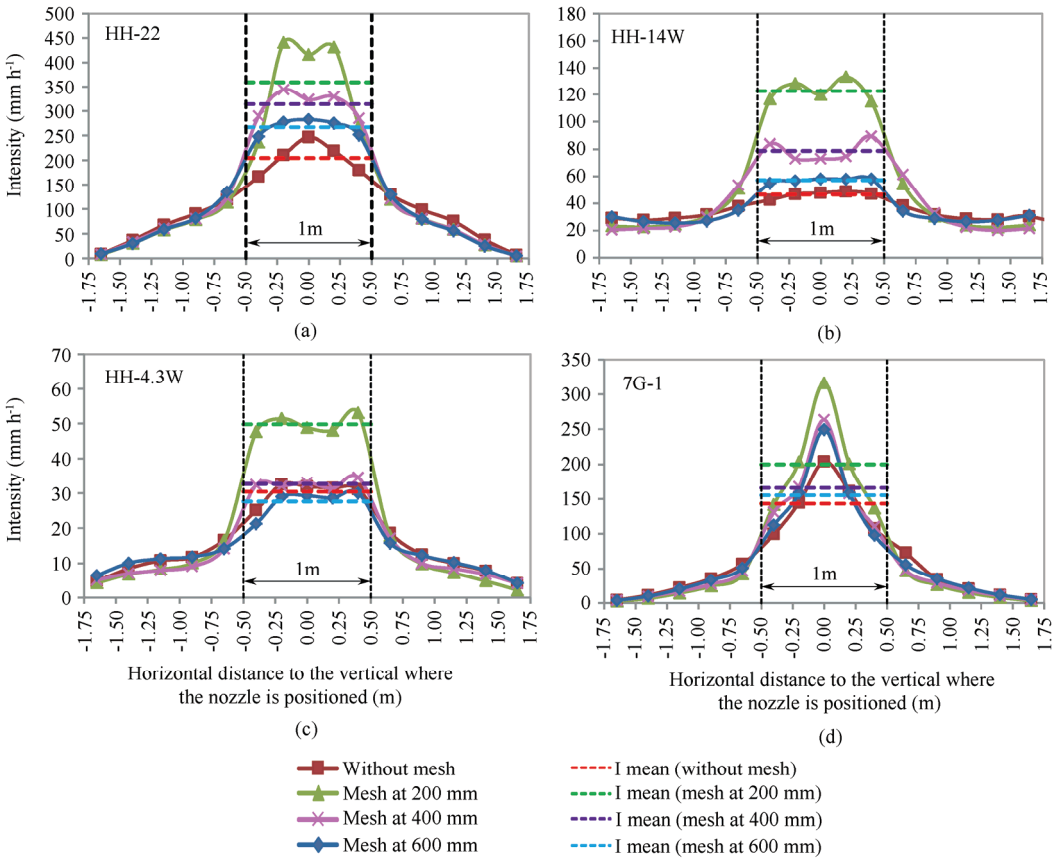

Fig. 4 Rainfall intensities observed along the 3.5 m diameter of the nozzle spray wetted circle, for simulations conducted without combining the nozzles with meshes and combining the nozzles with a plastic mesh (square aperture of 20 mm) that was positioned beneath the spray nozzles, at vertical distances of 200, 400 and 600 mm: (a) HH-22; (b) HH-14W; (c) HH-4.3W and (d) 7G-1 (Data are average values of 3 replicates)

Nozzles HH-22 and 7G-1 are the ones producing the highest intensities beneath the nozzle, which decreases strongly a short distance away (Fig. 4a and d); they also yield less uniform water distribution on the control plot.

Fig. 4 shows that the mean rainfall intensities were higher for meshes combined with the nozzles than for mesh-free simulations. The mesh used affects the distribution of the rainfall intensity generated by nozzles: it is responsible for concentrating the rainfall intensity on the area below the nozzle because most drops that hit the meshes will fall vertically underneath, although some drops can also be ejected away from the meshes by splash.

3.1.2 Meshes at different distances from the nozzle

The importance of the vertical distance adopted between the nozzle and the mesh underneath was assessed for the control plot; we tested distances of 200, 400 and 600 mm. Results show that, in general, this distance affects the mean rainfall intensity simulated, which tends to increase as this distance decreases (Fig. 5a). The corresponding wire thickness of the meshes are different (see Table 2) but this variable seems not to affect the results.

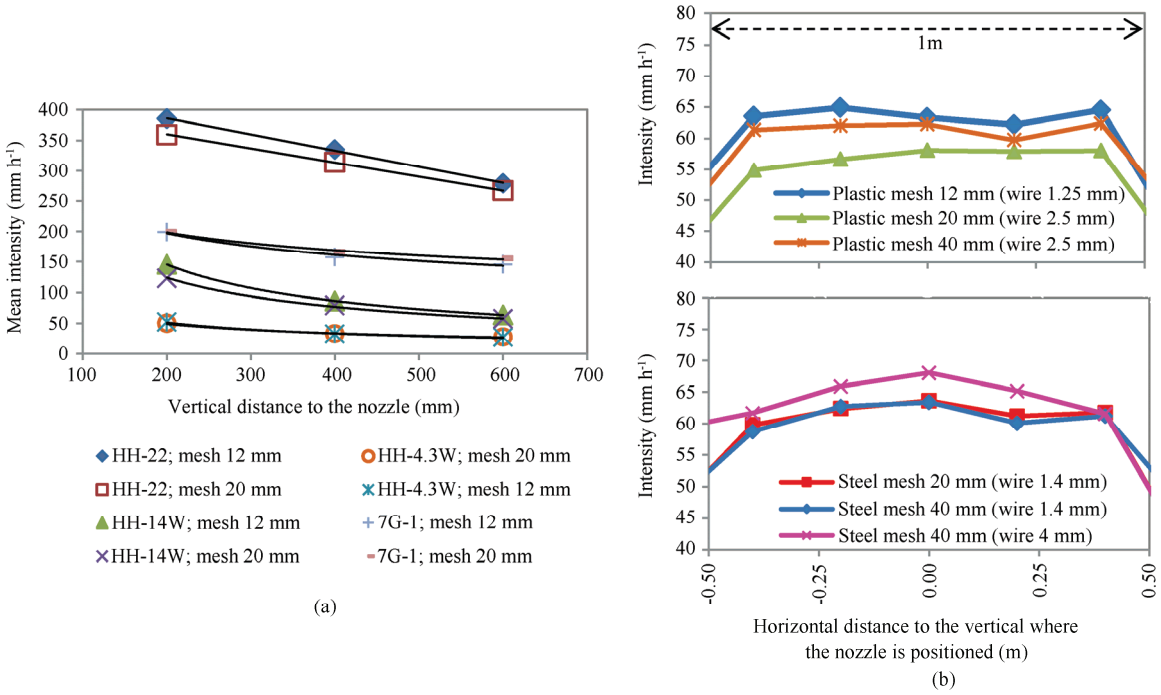

Fig. 5 (a) Mean rainfall intensities observed combining nozzles with plastic meshes (square aperture of 12 mm and 20 mm) as a function of the vertical distances between the meshes and the nozzle; data are average values for the control plot and lines are only indicative of trends. (b) Comparison between the rainfall intensities observed along the control plot when combining the spray nozzle HH-14W with plastic meshes (square apertures of 12, 20 and 40 mm) and steel meshes (square apertures of 20 mm and 40 mm); the distance between the mesh and the nozzle was 600 mm

3.1.3 Meshes made of two materials, different square apertures and thicknesses

The effect of the meshes' material (plastic and steel) was attempted by using only one nozzle type (HH-14W), one distance to the nozzle (600 mm), and two square apertures for both the plastic and steel meshes (20 mm or 40 mm).

Descriptive statistics of the measured rainfall intensities are given in Table 4. The mesh material (plastic and steel) seems not to influence much the measured rain intensities (Fig. 5b). The results obtained using plastic and steel meshes with different square apertures also show that the aperture of the meshes used seems not to affect significantly the intensity of the simulated rainfall (Fig. 5b). Also, there is no clear evidence of the impact of the wire thickness on the measured rain intensities.

3.2 *Diameter and fall speed of drops*

The diameter and fall speed of the raindrops was analysed for the 4 nozzles tested. The rainfall simulated without using meshes was compared to the rain produced when a plastic mesh (with a square aperture of 20 mm) was positioned at three distances from the nozzle (200, 400 and 600 mm).

Table 4 Descriptive statistics of rainfall intensities measured in the control plot, for nozzles combined with steel and plastic meshes. The spray nozzle type used was HH-14W and the vertical distance between the mesh and the nozzle was 600 mm. Data are for the 5 gauges in the control plot (Fig. 3c), 3-minute sampling time, and 3 replicates

	Meshes						
Material	Plastic wire			Steel wire			Without mesh
Square aperture (mm)	12	20	40	20	40	40	
Wire thickness (mm)	1.0-1.5	2.0-3.0	2.0-3.0	1.4	4.0	1.4	
Average (mm h^{-1})	63.7	57.1	61.5	61.8	64.5	61.2	46.6
Minimum (mm h^{-1})	62.2	54.9	59.7	59.8	61.6	58.8	42.6
Maximum (mm h^{-1})	64.9	58.1	62.4	63.6	68.1	63.4	48.7
Coef. variation	0.02	0.02	0.02	0.02	0.04	0.03	0.05
Coef. uniformity (%)	98.7	98.1	98.7	98.4	96.5	97.6	96.5

Results suggest that, overall, the presence of meshes increased the mass-weighted mean drop diameter (D_m) of the simulated rainfall; in Fig. 6a, the majority of points are located above the 1:1 line. The mass-weighted mean diameter of the drops simulated with all the nozzles without using meshes varied between 0.65 mm and 1.76 mm and between 0.73 mm and 2.69 mm when meshes were used.

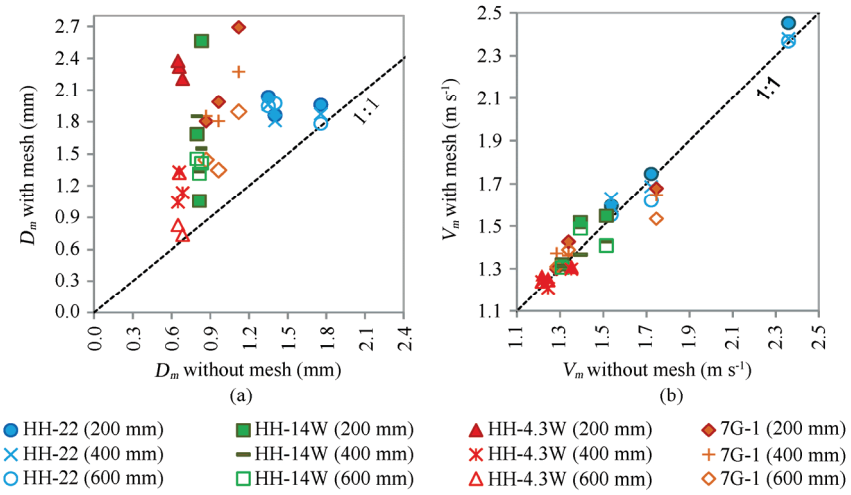

Fig. 6 Comparison of simulated raindrops' properties observed combining the spray nozzle with a plastic mesh (square aperture of 20 mm) and without mesh: (a) mass-weighted mean diameter; (b) mean fall speed. The spray nozzles tested are identified in the legend. The results are for meshes positioned at three vertical distances from the nozzles: 200, 400 and 600 mm
[The data were collected during 15 s (3 replicates) with a laser disdrometer positioned in three positions that correspond to the 3 data points for each combination nozzle type-distance (see Fig. 3d).]

The formation of larger drops that are caused by the meshes, in relation to the mesh-free simulations, increased the mass-weighted mean diameter of the simulated raindrops and lead to a broader range of drop sizes. This is illustrated in Fig. 7 that shows the effect of the plastic mesh (square aperture of 20 mm) on the rain simulations recorded just below the 4 nozzles. It is expected that water drops that hit the meshes will detach from it after growing up to a size at which its weight overcomes the surface tension force, thus the number of larger drops increases. We note that the increase in drop size caused by the meshes is less strong for the HH-22 nozzle; this is because the nozzle was nevertheless producing drops larger than the other nozzles, even without the meshes. In particular, just below the nozzle the maximum drop diameter recorded for this case was 6.25 mm. Other properties of the spray formed by this nozzle are discussed below.

The fine 7G-1 spray nozzle forms very small droplets, yielding a rather dense spray resembling fog. The expectation is that the smaller number of drops in the lowest drop size class reported by the laser disdrometer (Fig. 7d) in comparison to other nozzles (Fig. 7a, b and c) is explained, at least partly, by the lower size-limit detection for the drops (i.e. 0.125 mm diameter) which could lead to undersampling of small drops below this

limit. However, this effect, if present, does not affect the qualitative evaluation of the impact of meshes on changing the properties of the drops formed by this nozzle.

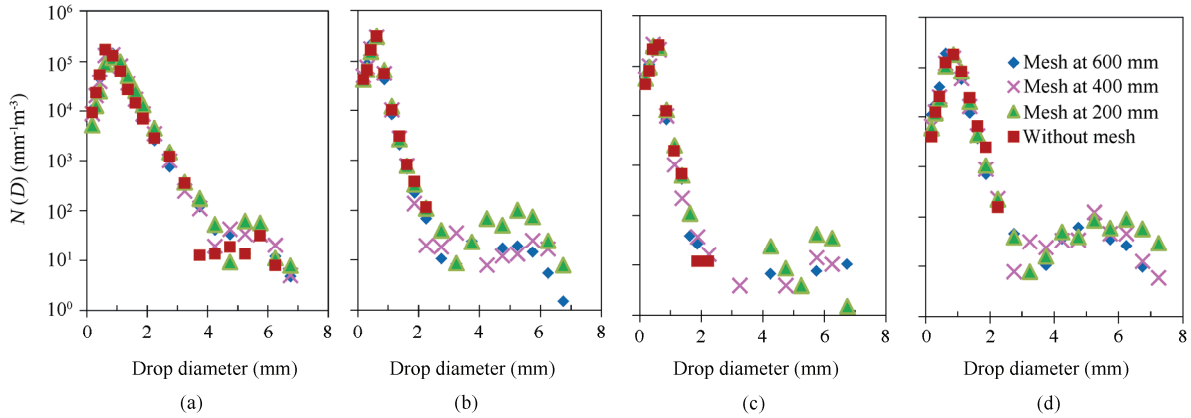

Fig. 7 Rain drop size distribution produced by spray nozzles combined with a plastic mesh (square aperture of 20 mm) and without mesh: (a) HH-22; (b) HH-14W; (c) HH-4.3W; (d) 7G-1 (The data were collected with the disdrometer positioned in the centered position, on the measuring plane, and the meshes were positioned at three distances from the nozzle.)

The drop fall speed seems not to be much affected by the presence of meshes. Fig. 6b shows that drop fall speed ranges from 1.2 m s^{-1} to 2.4 m s^{-1} for the mesh-free simulations and are between 1.2 m s^{-1} and 2.5 m s^{-1} for the simulations conducted with meshes. This figure shows that in 36% of the tests the fall speed was higher in the simulations using meshes, and smaller in 28% of them. Nevertheless, it might be expected that without meshes the fall speed is higher, because drops are forced out of the spray nozzles at high velocities, whereas drops that fall from meshes have an initial velocity of zero. However, despite the short fall distance from the mesh to the ground, the bigger drops that are formed due to the presence of meshes fall faster because of their greater mass; in addition, it is expected that the majority of drops fall to the target surface without hitting the mesh. Similar results were obtained for the plastic mesh of 12 mm aperture (Fig. 5b and Table 4).

4 Conclusions

A laboratory set-up was prepared to evaluate the impact of combining meshes with spray nozzles on rain simulations, with the meshes being positioned underneath the nozzles and intercepting the spray (i.e. the drops trajectories). The meshes were made of plastic and steel, with square apertures from 12 to 40 mm, installed at various vertical distances away from the nozzles. For the control plot, we report the following findings:

(i) Rainfall intensities

- In general, the meshes increased the mean rainfall intensity on the control plot, beneath the nozzle, as most raindrops that hit the meshes fall vertically underneath; nevertheless, this effect on the rain simulations is affected by the distance between the mesh and the nozzle.
- The mean rainfall intensity under the meshes increases as the distance between the meshes and the nozzles decreases; this is also explained by the drop concentration effect caused by the interception of the drop trajectories by the mesh.
- The meshes' material (plastic and steel), wire thickness and square apertures seem not to have much influence on the simulated rain properties; but the limited number of conditions studied restricts the analysis of results and hence the tests were not conclusive.

(ii) Raindrop properties

While intercepting the nozzle sprays, the meshes altered the simulated raindrops' properties. In particular, for the raindrops diameter and fall speed, the main findings were:

- The mass-weighted mean diameter of the simulated raindrops was higher when meshes were used, in relation to the simulations carried out without combining meshes and nozzles. Because spray nozzles generate typically small drop sizes and narrow drop size distributions, when meshes are combined with nozzles they promote the formation of bigger drops and the randomization of their landing positions;

– The mean fall speed of the simulated raindrops was similar for simulations carried out with and without meshes. Results suggest that overall the meshes might not have much influence on the mean fall speed because regardless of the presence of the meshes a large amount of drops still fall directly from the nozzle without hitting the meshes.

Thus, meshes can be used to alter the mean rainfall intensity produced by spray nozzles, and also the drop sizes. Note that by varying the operating nozzle pressure, which was kept constant in this exploratory work, the diameter and fall speed of drops can be changed. Indeed, lower nozzle pressures yield larger drops with lower fall speed, whereas higher pressures produce smaller drops with higher fall speed.

In this study no attempt was made to reproduce natural rainfall. Further research should be done to investigate how nozzle type, operating pressure and meshes can be used to adjust the characteristics of spray nozzle simulated rainfall to those of a specific natural rainfall.

Acknowledgements

The first author is grateful to the Foundation for Science and Technology (FCT) of the Portuguese Ministry of Education and Science for the financial support through a Doctoral Grant SFRH/BD/60213/2009. The laboratory experiments were supported by project PTDC/ECM/105446/2008, funded by FCT and by the Operational Programme 'Thematic Factors of Competitiveness' (COMPETE), shared by the European Regional Development Fund (ERDF).

References

Abd Elbasit, M. A. M., Yasuda, H., Salmi, A., & Anyoji, H. (2010). Characterization of rainfall generated by dripper-type rainfall simulator using piezoelectric transducers and its impact on splash soil erosion. *Earth Surface Processes and Landforms*, *35*(4), 466-475.

Arnaez, J., Lasanta, T., Ruiz-Flaño, P., & Ortigosa, L. (2007). Factors affecting runoff and erosion under simulated rainfall in Mediterranean vineyards. *Soil and Tillage Research*, *93*(2), 324-334.

Battany, M. C., & Grismer, M. E. (2000). Development of a portable field rainfall simulator for use in hillside vineyard runoff and erosion studies. *Hydrological Processes*, *14*(6), 1119-1129.

Bowyer-Bower, T. A. S., & Burt, T. P. (1989). Rainfall simulators for investigating soil response to rainfall. *Soil Technology*, *2*(1), 1-16.

Cerdà, A., Ibáñez, S., & Calvo, A. (1997). Design and operation of a small and portable rainfall simulator for rugged terrain. *Soil Technology*, *11*(2), 163-170.

Christiansen, J. E. (1941). The uniformity of application of water by sprinkler systems. *Agricultural Engineering*, *22*(3), 89-92.

Clarke, M. A., & Walsh, R. P. D. (2007). A portable rainfall simulator for field assessment of splash and slopewash in remote locations. *Earth Surface Processes and Landforms*, *32*(13), 2052-2069.

de Lima, J. L. M. P., & Singh, V. P. (2003). Laboratory experiments on the influence of storm movement on overland flow. *Physics and Chemistry of the Earth, 28*(6), 277-282.

de Lima, J. L. M. P., Singh, V. P., & de Lima, M. I. P. (2003). The influence of storm movement on water erosion: storm direction and velocity effects. *Catena*, *52*(1), 39-56.

de Lima, J. L. M. P., Souza, C. S., & Singh, V. P. (2008). Granulometric characterization of sediments transported by surface runoff generated by moving storms. *Nonlinear Processes in Geophysics*, *15*(6), 999-1011.

de Lima, J. L. M. P., Carvalho, S. C. P., & de Lima, M. I. P. (2013). Rainfall simulator experiments on the importance of when rainfall burst occurs during storm events on runoff and soil loss. *Zeitschrift für Geomorphologie, 57*(1), 91-109.

de Ploey, J. (1981). The ambivalent effects of some factors of erosion. *Mémoires de l'Institut de Géologie de l'Université de Louvain*, *31*, 171-181.

Erpul, G., Gabriels, D., & Janssens, D. (1998). Assessing the drop size distribution of simulated rainfall in a wind tunnel. *Soil and Tillage Research*, *45*(3), 455-463.

Esteves, M., Planchon, O., Lapetite, J. M., Silvera, N., & Cadet, P. (2000). The “emire” large rainfall simulator: design and field testing. *Earth Surf. Process. Landforms*, *25*, 681-690.

Fernández-Gálvez, J., Barahona, E., & Mingorance, M. D. (2008). Measurement of infiltration in small field plots by a portable rainfall simulator: application to trace-element mobility. *Water, Air, and Soil Pollution*, *191*(1-4), 257-264.

Fister, W., Iserloh, T., Ries, J. B., & Schmidt, R. G. (2012). A portable wind and rainfall simulator for in situ soil erosion

measurements. *Catena*, *91*, 72-84.

Holden, J., & Burt, T. P. (2002). Infiltration, runoff and sediment production in blanket peat catchments: implications of field rainfall simulation experiments. *Hydrological Processes*, *16*(13), 2537-2557.

Humphry, J. B., Daniel, T. C., Edwards, D. R., & Sharpley, A. N. (2002). A portable rainfall simulator for plot-scale runoff studies. *Applied Engineering in Agriculture*, *18*(2), 199-204.

Kamphorst, A. (1987). A small rainfall simulator for the determination of soil erodibility. *Netherlands Journal of Agricultural Science*, *35*(3), 407-415.

Kincaid, D. C. (1996). Spraydrop kinetic energy from irrigation sprinklers. *Transactions of the ASAE*, *39*(3), 847-853.

Krajewski, W. F., Kruger, A., Caracciolo, C., Golé, P., Barthes, L., Creutin, J. D., ... & Vinson, J. P. (2006). DEVEX-disdrometer evaluation experiment: Basic results and implications for hydrologic studies. *Advances in Water Resources*, *29*(2), 311-325.

Lascelles, B., Favis-Mortlock, D. T., Parsons, A. J., & Guerra, A. J. (2000). Spatial and temporal variation in two rainfall simulators: implications for spatially explicit rainfall simulation experiments. *Earth Surface Processes and Landforms*, *25*(7), 709-721.

Marques, M. J., Bienes, R., Jiménez, L., & Pérez-Rodríguez, R. (2007). Effect of vegetal cover on runoff and soil erosion under light intensity events. Rainfall simulation over USLE plots. *Science of the Total Environment*, *378*(1), 161-165.

Meyer, L. D., & McCune, D. L. (1958). Rainfall simulator for runoff plots. *Agric. Eng*, *39*(10), 644-648.

Munn, J. R., & Huntington, G. L. (1976). A portable rainfall simulator for erodibility and infiltration measurements on rugged terrain. *Soil Science Society of America Journal*, *40*(4), 622-624.

Mutchler, C. K., & Hermsmeier, L. F. (1965). A review of rainfall simulators. *Trans. ASAE*, *8*(1), 67-68.

Parsons, A. J., & Stone, P. M. (2006). Effects of intra-storm variations in rainfall intensity on interrill runoff and erosion. *Catena*, *67*(1), 68-78.

Potter, T. L., Truman, C. C., Strickland, T. C., Bosch, D. D., Webster, T. M., Franklin, D. H., & Bednarz, C. W. (2006). Combined effects of constant versus variable intensity simulated rainfall and reduced tillage management on cotton preemergence herbicide runoff. *Journal of Environmental Quality*, *35*(5), 1894-1902.

Ries, J. B., Seeger, M., Iserloh, T., Wistorf, S., & Fister, W. (2009). Calibration of simulated rainfall characteristics for the study of soil erosion on agricultural land. *Soil and Tillage Research*, *106*(1), 109-116.

Schindler Wildhaber, Y., Bänninger, D., Burri, K., & Alewell, C. (2012). Evaluation and application of a portable rainfall simulator on subalpine grassland. *Catena*, *91*, 56-62.

Spraying Systems Co. (2013). Industrial Hydraulic Spray Products, Catalog 75 HYD, USA.

Thies, A. (2007). Instruction for Use 021341/08/07. Laser Precipitation Monitor 5.4110.xx.x00 V2.4x STD. 64 pp.

Tossell, R. W., Rudraz, R. P., & Wall, G. J. (1987). A portable rainfall simulator. *Canadian Agricultural Engineering*, *29*(2), 155-162.

Ulbrich, C. W. (1983). Natural variations in the analytical form of the raindrop size distribution. *Journal of Climate and Applied Meteorology*, *22*(10), 1764-1775.